

Mechanism of formation of ultrashallow thermal donors in carbon-doped oxygen-rich monocrystalline silicon preannealed to introduce hydrogen

This content has been downloaded from IOPscience. Please scroll down to see the full text.

2015 Jpn. J. Appl. Phys. 54 101302

(<http://iopscience.iop.org/1347-4065/54/10/101302>)

View [the table of contents for this issue](#), or go to the [journal homepage](#) for more

Download details:

IP Address: 157.118.208.83

This content was downloaded on 23/09/2015 at 10:00

Please note that [terms and conditions apply](#).

Mechanism of formation of ultrashallow thermal donors in carbon-doped oxygen-rich monocrystalline silicon preannealed to introduce hydrogen

Akito Hara and Teruyoshi Awano

Faculty of Engineering, Tohoku Gakuin University, Tagajo, Miyagi 985-8537, Japan

E-mail: akito@mail.tohoku-gakuin.ac.jp

Received April 23, 2015; accepted July 25, 2015; published online September 18, 2015

We previously reported on ultrashallow thermal donors (USTDs) in carbon-doped oxygen-containing monocrystalline silicon (Czochralski-grown, CZ-Si) crystals that were preannealed to introduce hydrogen at 1300 °C, and then annealed at 480 °C. In this study, the formation mechanism of the USTDs was evaluated. It was observed that an increase in the intensity of USTDs leads to a reduction in that of hydrogen-related shallow thermal donors [STD(H)s], and the sum of the area intensities of the lines in the transmission spectra of USTDs and STD(H)s is nearly constant when the silicon crystals are annealed for longer than 10 h at 480 °C. We also found some thermally activated processes linked to the formation of USTDs. We thus conclude that the mechanism is composed of the high-speed formation of STD(H)s in the first stage and carbon modulation of the electronic structure of STD(H)s in the second stage. © 2015 The Japan Society of Applied Physics

1. Introduction

We previously reported on ultrashallow thermal donors (USTDs) in carbon- and nitrogen-doped monocrystalline Czochralski-grown silicon (CZ-Si) crystals after annealing at 480 or 600 °C.¹⁾ Many new lines between 100–300 cm⁻¹ in the transmission spectra, distinct from those arising from hydrogen-related shallow thermal donors [STD(H)]^{2,3)} and nitrogen oxygen (NO) complexes,⁴⁻⁷⁾ have been attributed to the optical transition of hydrogen-like donors from the ground state to the excited state. Some of these show negative central-cell correction and, to the best of our knowledge, correspond to the shallowest energy levels among all previously reported hydrogen-like donors in Si crystals.¹⁾ However, it has been pointed out that the samples analyzed in Ref. 1 were contaminated with hydrogen.^{8,9)} In another study,¹⁰⁾ the annealing gas was carefully controlled. Table I shows the peak positions observed in the Ref. 10, which correspond to USTDs-1 to -5 in Ref. 1, hydrogen-related thermal donors [STD(H)s]-2 and -3, and USTDs-1' and -2'. We observed that the spectral lines identified as USTDs-1 to -5 formed at 480 °C in Ref. 1 were also formed in carbon-doped monocrystalline CZ-Si, which was preannealed to introduce hydrogen, and that the nitrogen doping status was independent of the presence of USTDs-1 to -5.¹⁰⁾ Additionally, USTDs-1' and -2', which are dependent on nitrogen concentration, were also generated in the carbon- and nitrogen-doped CZ-Si crystals at approximately 600 °C.¹⁰⁾ The peak positions of USTDs-1 to -5 were clearly different from those of USTDs-1' and -2', as shown in Table I.

Solar-cell-grade multicrystalline silicon (mc-Si) includes high concentrations of contaminations during solidification. Carbon, oxygen, and nitrogen are typical light-mass contaminants in mc-Si. Hydrogen is also an important element in mc-Si solar cells because hydrogen gas is used in thin-film growth methods, which are frequently applied in device fabrication.

From the viewpoint of light-mass impurities, the major difference between mc-Si and CZ-Si for large-scale integration (LSI) is the concentrations of carbon and nitrogen. The carbon and nitrogen concentrations in LSI-Si are controlled to levels below the detection limits of the elements ($[C] < 10^{16} \text{ cm}^{-3}$ and $[N] < 10^{14} \text{ cm}^{-3}$). On the other hand, the

Table I. 1s–2p_± transition of USTDs, STD(H)s and USTDs-1' and 2'.¹⁰⁾

Donor	2p _± (cm ⁻¹)	Donor	2p _± (cm ⁻¹)	Donor	2p _± (cm ⁻¹)
USTD-1	173.3	STD(H)-2	246.9	USTD-1'	216.0
USTD-2	175.8	STD(H)-3	241.1	USTD-2'	192.1
USTD-3	179.6				
USTD-5	202.4				

carbon and nitrogen concentrations in mc-Si are on the order of 10¹⁷ and 10¹⁵ cm⁻³, respectively. It has been reported that complex centers or aggregative defects composed of light-mass elemental impurities degrade the yield and reliability of Si-LSI. High concentrations of light-mass elemental impurities in mc-Si are thus also expected to have negative effects on the performance, yield, and reliability of mc-Si solar cells. Therefore, the evaluation of reactions between these impurities in mc-Si is necessary for the development of materials for mc-Si solar cells.^{11,12)}

In this study, we evaluated the formation of USTDs-1 to -5 at various durations and temperatures of USTD formation annealing, using carbon-doped CZ-Si crystals that were preannealed to introduce hydrogen.¹³⁻¹⁵⁾ As we evaluated the formation mechanism of USTDs using non-nitrogen-doped CZ-Si, that USTDs-1' and -2' is beyond the scope of this study.

2. Experimental methods

Two types of III- and V-dopant-free CZ-Si crystals were used as precursors. The first was a low-carbon-content CZ-Si, with $[C] < 1 \times 10^{16} \text{ cm}^{-3}$ and $[O] = 1.6 \times 10^{18} \text{ cm}^{-3}$ (old American Society for Testing and Materials), and the second was carbon-doped CZ-Si with $[C] = (1.8-2.3) \times 10^{17} \text{ cm}^{-3}$ and $[O] = 1.6 \times 10^{18} \text{ cm}^{-3}$. The carbon-doped CZ-Si was grown from carbon-powder-doped molten Si. Samples with a thickness of 2.0 mm were prepared; far-infrared (far-IR) optical absorption measurements were performed on beam-line 6B (resolution, 0.5 cm⁻¹, temperature, 8–10 K) at the UVSOR facility of the Institute for Molecular Science.

Figure 1 shows the optical transmission spectra of the carbon-doped CZ-Si crystals. The first sample was annealed

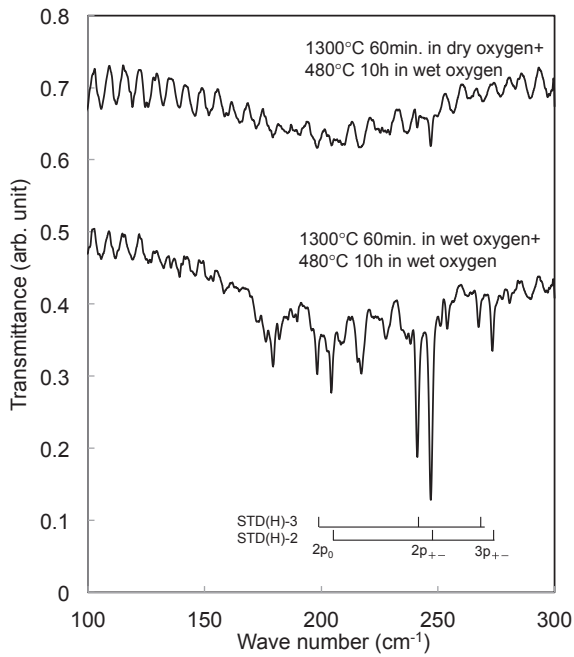


Fig. 1. Transmission spectra for STD(H)s and USTDs. The first Si sample was annealed at 1300 °C for 60 min in wet oxygen, quenched in air, and further annealed at 480 °C for 10 h in wet oxygen (hydrogen-doped Si). The second sample was annealed at 1300 °C for 60 min in dry oxygen, quenched in air, and further annealed at 480 °C for 10 h in wet oxygen.

at 1300 °C for 60 min in wet oxygen, quenched in air, and then annealed further at 480 °C for 10 h in wet oxygen. The second sample was annealed at 1300 °C for 60 min in dry oxygen, quenched in air, and then annealed further at 480 °C for 10 h in wet oxygen. In these processes, the wet oxygen was prepared by passing dry oxygen gas through boiling water so as to include moisture in the atmosphere. The difference in the intensities of the peaks correlating to STD(H)s is evident. It has been reported that STD(H)s are donors with hydrogen-like energy levels and are generated in hydrogen-doped CZ-Si crystals at approximately 450 °C.^{2,3,8,9} Figure 1 indicates that it is possible to introduce hydrogen into CZ-Si by preannealing the Si crystals at 1300 °C for 60 min in wet oxygen. Herein, monocrystalline Si prepared by the above-described hydrogen doping process is referred to as hydrogen-doped Si. This hydrogen doping method is a slight modification of the method proposed by Martynov et al.³⁾

3. Results

Figure 2 shows the behavior of USTDs and STD(H)s observed in the carbon- and hydrogen-doped CZ-Si annealed at 480 °C in wet oxygen for various durations. In this study, we divided USTDs-1 to -5 into two groups of USTD group 1 (USTD G1) and USTD group 2 (USTD G2), as shown in Fig. 2, in order to simplify the analysis of the formation of USTDs. Here, USTDs-1 to -3 and USTD-5 were classified into USTD G1 and USTD G2, respectively.

We think that USTDs-1, -2, and -3 are a family of donor species, because their energy levels are very similar. The USTDs-1 and -2, with shallow energy levels, gradually reduce in intensity, while USTD-3 with the deepest energy level survives after long-term annealing. This behavior differs from conventional cluster (family) donors, such as thermal double donors (TDDs) and NO complex donors, in

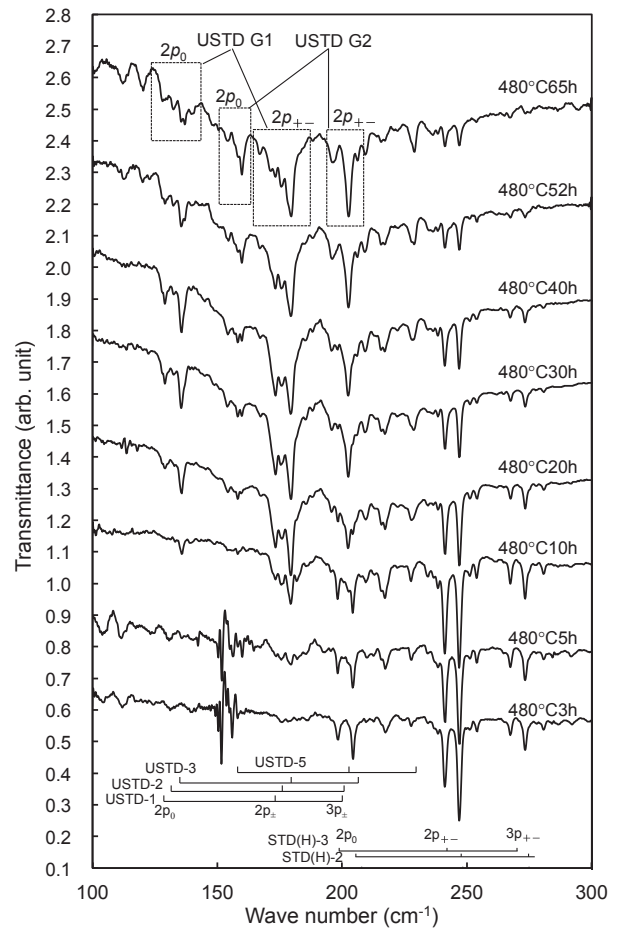


Fig. 2. Variation in USTD and STD(H) spectral intensities in carbon- and hydrogen-doped monocrystalline CZ-Si as a function of annealing duration at 480 °C in wet oxygen.

which the donors with shallower energy levels are more likely to survive after long annealing times. In contrast, one strong line in the transmission spectra, corresponding to USTD-5, dominates in USTD G2 from the initial stages of annealing. The energy level of USTD-5 differs from that of USTD G1, thus, its the assignment to a different group.

The STD(H) spectral line intensities are high even after short-term annealing for 3 h, and are maximum after 10 h annealing. This indicates that the formation speed of STD(H)s is much higher than that of USTDs. Notably, the STD(H) lines decrease in intensity as the annealing continues beyond 10 h.

Figure 3 shows the spectral intensity of USTD and STD(H) lines observed in non-carbon-doped and hydrogen-doped CZ-Si after annealing for 10 and 48 h at 480 °C. The USTD lines do not appear even after long-term annealing for 48 h, while the intensity of the STD(H) lines after 48 h is nearly equal to that after 10 h annealing. This is markedly different from the annealing behavior of STD(H)s in the carbon- and hydrogen-doped CZ-Si, as shown in Fig. 2. Carbon impurities can thus be concluded to be necessary in the generation of USTD spectral lines and reduction in the intensity of STD(H) spectral lines.

Figure 4 shows the annealing temperature dependence of the intensity of USTD and STD(H) lines in carbon- and hydrogen-doped CZ-Si. The annealing duration was fixed at 40 h, but different annealing temperatures of 450, 480, and

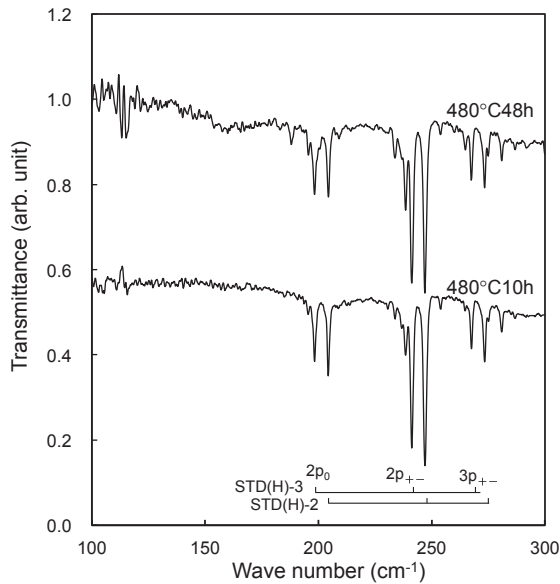


Fig. 3. Intensities of STD(H) and USTD spectral lines formed in hydrogen-doped, non-carbon-doped CZ-Si after annealing for 10 and 48 h at 480 °C.

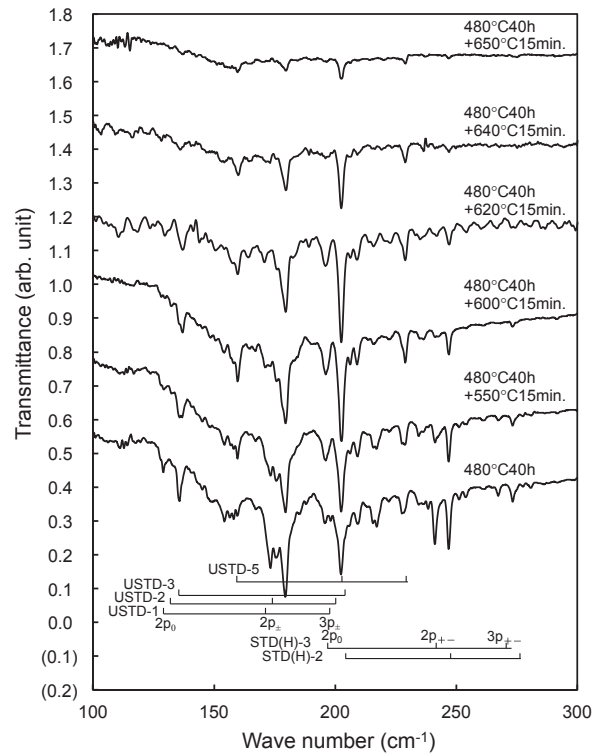


Fig. 5. Variation in the intensities of USTD and STD(H) spectral lines formed in carbon- and hydrogen-doped CZ-Si after annealing at 480 °C for 40 h followed by 15 min annealing at higher temperatures, as a function of wet-oxygen annealing temperature.

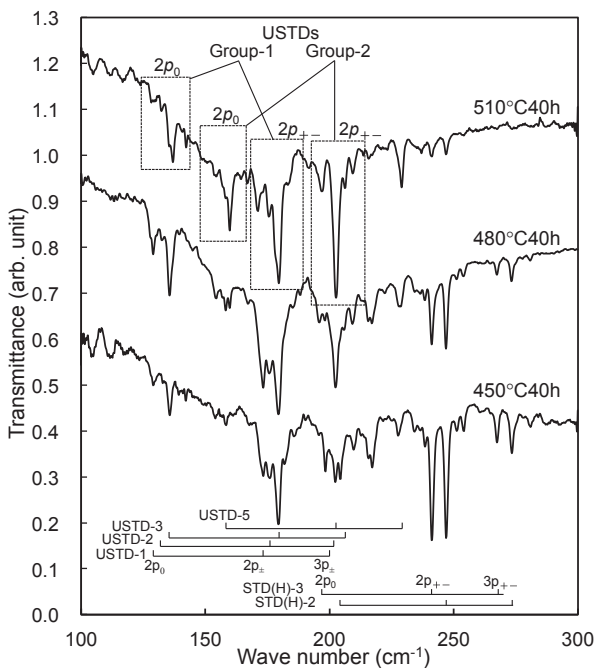


Fig. 4. Variation in intensities of USTD and STD(H) spectral lines formed in carbon- and hydrogen-doped monocrystalline CZ-Si after annealing for 40 h at 450, 480, and 510 °C in wet oxygen.

510 °C were used. The USTD lines for samples annealed at 450 °C appear to be equivalent to those for samples annealed at 480 °C for 20 h, as shown in Fig. 2. On the other hand, the USTD lines of samples annealed at 510 °C for 40 h appear to be similar to those of the samples annealed at 480 °C for 65 h, compared with the other lines of USTDs at 480 °C. Thus, the USTD lines of samples with shorter annealing durations at high temperatures are similar to those of samples with longer annealing durations at low temperatures; this indicates that thermally activated processes are linked with the formation of USTDs. Figure 4 also indicates that two

USTD spectral lines become dominant as the annealing temperature increases. This is consistent with the results shown in Fig. 2.

Figure 5 shows the variation in the intensity of USTD and STD(H) lines in carbon- and hydrogen-doped CZ-Si after annealing at 480 °C for 40 h followed by 15 min annealing at higher temperatures. The figure shows that the USTDs-1 and -2 lines gradually decrease in intensity as the second-phase annealing temperature increases, and at the highest temperatures, only USTDs-3 and -5 lines are observed. This is consistent with the results in Figs. 2 and 4.

To investigate the generation of USTDs and the reduction of STD(H)s at 480 °C for various annealing times, we examined the variations in area intensity of spectral peaks correlating to USTD G1, USTD G2, and STD(H)s. For the area intensity of USTD G1, $1s-2p_{\pm}$ spectral lines were applied, while for the area intensity of USTD G2, $1s-2p_0$ lines were applied. Because the $1s-3p_{\pm}$ spectral lines of USTD G1 and the $1s-2p_0$ lines of the STD(H)s both overlap with the $1s-2p_{\pm}$ lines of USTD G2, we selected the $1s-2p_0$ lines for USTD G2. According to the effective-mass theory,¹⁶⁾ the intensity ratio of $1s-2p_0$ to $1s-2p_{\pm}$ lines should be 4 : 10. Thus, we determined the area intensity of the $1s-2p_{\pm}$ lines of USTD G2 to be 2.5 times that of the $1s-2p_0$ lines of USTD G2. The area intensity of the $1s-2p_{\pm}$ STD(H) lines was obtained using the two main peaks and five satellite lines. Figure 6 shows a summary of the variation in area intensity of the $1s-2p_{\pm}$ lines of USTD G1, USTD G2, and STD(H)s, as well as the sum of these intensities as a function of annealing time at 480 °C. The sum of the area intensities of USTDs and STD(H)s seems to show a weak dependence

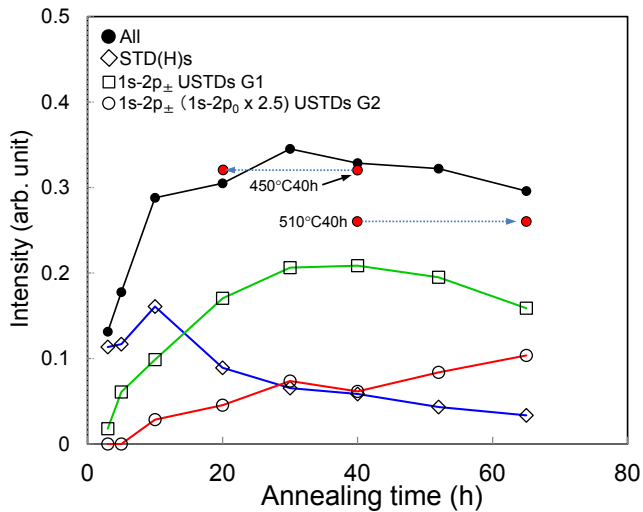


Fig. 6. (Color online) Variation in the intensities of spectral line areas for STD(H)s, USTD G1, and USTD G2, and their sum as a function of annealing duration at 480 °C. This figure includes data points of samples annealed at 450 °C or 510 °C for 40 h.

on annealing duration at 480 °C for durations greater than 10 h. The area intensities for the sum of the spectral lines of the USTDs and STD(H)s at 450 and 510 °C after 40 h from Fig. 4 are also plotted in Fig. 6. We noted earlier that the shapes of the spectral peaks corresponding to the USTDs and STD(H)s formed by annealing at 450 °C for 40 h are similar to those formed by annealing at 480 °C for 20 h. On the other hand, the spectra of samples annealed at 510 °C for 40 h are similar to those of samples annealed at 480 °C for 65 h. Therefore, the two data sets are also plotted for each corresponding annealing duration at 480 °C.

4. Discussion

The formation speed of the STD(H)s is clearly very high, because the STD(H) lines become obvious after 3 h annealing and are maximum after 10 h annealing at 480 °C, as shown in Fig. 2. Thus, we conclude that nearly all STD(H)s are generated within the first 10 h of annealing. As the line intensities of the USTDs increase, the line intensities of the STD(H)s decrease; the sum of the USTD and STD(H) line areas remains approximately constant for annealing durations exceeding 10 h at 480 °C. This indicates that the STD(H)s change to USTDs with prolonged annealing.

According to our proposed formation mechanism, the sum of the USTDs and STD(H)s depends on the amount of STD(H)s generated during the initial annealing stage. Because of the high formation speed of the STD(H)s, the diffusion of hydrogen is expected to be the rate-limiting process for the formation of STD(H)s. The hydrogen diffusion coefficient is very large and the activation energy for migration is very small within CZ-Si. Thus, the number of STD(H)s generated during the initial stage of annealing at 450 °C will be nearly the same for that generated during annealing at 480 °C. This explains the similarity in the sums of the signal intensities of the USTDs and STD(H)s of samples annealed at 450 °C after 40 h and those annealed at 480 °C for 20 h.

In contrast, the sum of the signal intensities of the USTDs and STD(H)s of samples annealed at 510 °C for 40 h is

lower than that of the samples annealed at 480 °C. Since the dissolution of STD(H)s occurs as in parallel with the formation of STD(H)s with increasing annealing temperature, the total amount of STD(H)s formed at the initial annealing stage at 510 °C decreases to less than that formed at 480 °C. Similar phenomena have been reported for NO complex donors, wherein the amount of NO complexes decreased with increasing annealing temperature.⁶⁾ Therefore, the sum of the line area of USTDs and STD(H)s of samples annealed at 510 °C for 40 h is lower than that for samples annealed at 480 °C. The effects of other hydrogen reaction processes must also be considered, especially at high temperatures, such as diffusion into atmosphere from the surface and gettering to oxygen precipitates formed during annealing. These factors contribute to the mechanism of the reduction in the sum of the line area of USTDs and STD(H)s formed at 510 °C.

The lower formation speed of USTDs indicates the existence of a rate-limiting process. This is clearly a thermally activated process, because the formation speed of USTDs is higher at high annealing temperatures and lower at low annealing temperatures, as shown in Fig. 4. Carbon and silicon are both group IV elements. Thus, it is reasonable to assume that carbon acts as a modulator of STD(H)s by replacing Si, which constitutes the core structure of STD(H)s. Generally, carbon occupies substitutional lattice sites; therefore, the diffusion coefficient of substitutional carbon (D) is very small, as given by $D = 1.9 \exp(-3.2eV/k_B T) \text{ cm}^2/\text{s}$.¹⁷⁾ This diffusion coefficient limits the diffusion length to far less than the atomic radius of Si when Si is annealed for 40 h at 480 °C. However, the D for interstitial or interstitialcy carbons is expected to be significantly larger than the above-mentioned value. It is well known that the presence of carbon enhances the formation of SiO₂ precipitates,¹⁷⁾ which in turn eject self-interstitial Si from the host lattice. The self-interstitial Si replaces the substitutional carbon in order to occupy the substitutional Si site, resulting in the formation of an interstitial carbon. Thus, we can propose a reasonable model for the formation mechanism of USTDs. The fast-forming STD(H)s, whose formation is completed during the initial annealing stage, are transformed into USTDs during long-term annealing by combining with carbon, which migrates via interstitial or interstitialcy mechanisms. Thus, the intensities of STD(H) and USTD lines simultaneously decrease and increase, respectively. Because the migration of interstitial or interstitialcy carbons and the generation of such carbons are thermally activated processes, this mechanism does not contradict the experimental results.

The direct observation of the existence of isolated interstitial carbons by IR analysis, photoluminescence (PL) analysis, or other methods, may support the proposed formation model. However, this observation seems to be difficult, because, according to electron irradiation experiments, interstitial carbon easily forms complex defects combining with carbon and other impurities.^{18,19)} This behavior of interstitial carbon also indicates that, if STD(H)s exist in Si crystals, the interstitial carbon interacts with STD(H)s, resulting in the formation of USTDs.

Since two main strong peaks exist for STD(H)s, which are mapped to species STD(H)s-2 and -3, it seems that the number of main peaks of USTDs would be reduced to two if

the proposed USTDs formation model is correct. Only two USTD lines, USTDs-3 and -5, were dominant after long-term annealing at 480 °C or at high-temperature annealing above 480 °C (see Figs. 2, 4, and 5); this indicates a correlation between STD(H)s and USTDs and supports the proposed formation model.

The intensity of USTD-5 lines continues to increase with increasing annealing duration, while that of USTD-3 lines decreases with annealing durations exceeding 40 h, as shown in Fig. 6. This may indicate a correlation between species USTDs-3 and -5. However, more experimentation is necessary to determine the interactions between them.

Here, we discuss another formation mechanism of USTDs. It is well known that carbon oxygen (CO) complexes²⁰⁾ are formed in carbon-doped CZ-Si crystals; thus, the following process may be a candidate for the formation mechanism of USTDs. In the initial stage, CO complexes form slowly; subsequently, the hydrogen atoms in STD(H)s dissolve, and finally, the dissolved hydrogen atoms migrate to the CO complexes, modifying them into USTDs. However, this model can be excluded because the amount of STD(H)s does not change even after long-term annealing at 480 °C, as shown in Fig. 3.

Åberg et al.²¹⁾ also observed the existence of USTDs by using deep-level transient spectroscopy (DLTS), a method very sensitive to surface defects. They found the existence of defects with shallow energy levels of 25 meV below the conduction band around the surface region. If we assume that the USTDs investigated here and in the previous report of Åberg et al. are identical, we must conclude that the samples investigated by Åberg et al. were contaminated with carbon and hydrogen; both of these impurities are indispensable to the formation of USTDs. However, we cannot speculate further on the origin of USTDs observed by the separate research groups, because both the properties of the initial Si and the annealing atmosphere used in the two studies differed.

5. Conclusions

We proposed a formation mechanism for USTDs in carbon- and hydrogen-doped monocrystalline CZ-Si crystals during annealing at 480 °C. In the first stage, STD(H)s form at a high rate; in the second stage, carbon diffuses via an interstitial

or interstitial mechanism and modulates the electronic structure of STD(H)s by combining with them to form the USTDs.

Acknowledgements

This study was partly conducted under the Joint Studies Program of the Institute for Molecular Science and the Japan Society for the Promotion of Science [Grant-in-Aid for Scientific Research (C), No. 25420339].

- 1) A. Hara, *Jpn. J. Appl. Phys.* **34**, 3418 (1995).
- 2) R. C. Newman, J. H. Tucker, N. G. Semaltianos, E. C. Lightowers, T. Gregorkiewicz, I. S. Zevenbergen, and C. A. J. Ammerlaan, *Phys. Rev. B* **54**, R6803 (1996).
- 3) Y. V. Martynov, T. Gregorkiewicz, and C. A. J. Ammerlaan, *Phys. Rev. Lett.* **74**, 2030 (1995).
- 4) M. Suezawa, K. Sumino, H. Harada, and T. Abe, *Jpn. J. Appl. Phys.* **25**, L859 (1986).
- 5) M. Suezawa, K. Sumino, H. Harada, and T. Abe, *Jpn. J. Appl. Phys.* **27**, 62 (1988).
- 6) A. Hara, T. Fukuda, T. Miyabo, and I. Hirai, *Appl. Phys. Lett.* **54**, 626 (1989).
- 7) A. Hara, T. Fukuda, T. Miyabo, and I. Hirai, *Jpn. J. Appl. Phys.* **28**, 142 (1989).
- 8) R. E. Pritchard, M. J. Ashwin, J. H. Tucker, R. C. Newman, E. C. Lightowers, T. Gregorkiewicz, I. S. Zevenbergen, C. A. J. Ammerlaan, R. Falster, and M. J. Binns, *Semicond. Sci. Technol.* **12**, 1404 (1997).
- 9) R. C. Newman, M. J. Ashwin, R. E. Pritchard, and J. H. Tucker, *Phys. Status Solidi B* **210**, 519 (1998).
- 10) A. Hara, T. Awano, Y. Ohno, and I. Yonenaga, *Jpn. J. Appl. Phys.* **49**, 050203 (2010).
- 11) C. Peng, H. Zhang, M. Stavola, V. Yelundur, A. Rohatgi, L. Carnel, M. Seacrist, and J. Kalejs, *J. Appl. Phys.* **109**, 053517 (2011).
- 12) H. Zhang, M. Stavola, and M. Seacrist, *J. Appl. Phys.* **114**, 093707 (2013).
- 13) A. Hara and T. Awano, UVSOR Activity Rep. **2012**, 103 (2013).
- 14) A. Hara and T. Awano, UVSOR Activity Rep. **2013**, 88 (2014).
- 15) A. Hara and T. Awano, Tech. Dig. 6th World Conf. Photovoltaic Energy Conversion, 2014, p. 659.
- 16) W. Kohn, *Solid State Physics* (Academic Press, New York, 1957) Vol. 5, p. 257.
- 17) F. Shimura, *Semiconductor Silicon Crystal Technology* (Academic Press, San Diego, CA, 1988).
- 18) L. W. Song, X. D. Zhan, B. W. Benson, and G. D. Watkins, *Phys. Rev. B* **42**, 5765 (1990).
- 19) X. D. Zhan and G. D. Watkins, *Phys. Rev. B* **47**, 6363 (1993).
- 20) R. C. Newman and R. S. Smith, *J. Phys. Chem. Solids* **30**, 1493 (1969).
- 21) D. Åberg, M. K. Linnarsson, B. G. Svensson, T. Hallberg, and J. L. Lindström, *J. Appl. Phys.* **85**, 8054 (1999).